Liquid Crystals

Publication details, including instructions for authors and subscription information:
http://www.informaworld.com/smpp/title~content=t713926090

Hysteresis behaviour of the nematic-cholesteric phase transition for liquid crystals on polyimide films without use of the rubbing technique

Yoshikazu Yabe[a]; Dae-Shik Seo[b]
[a] Development Engineering Department, Engineering Division, Fujitsu Kiden Limited, Tokyo, Japan [b] Division of Electronic and Information Engineering, Faculty of Technology, Tokyo University of Agriculture and Technology, Tokyo, Japan

To cite this Article Yabe, Yoshikazu and Seo, Dae-Shik(1994) 'Hysteresis behaviour of the nematic-cholesteric phase transition for liquid crystals on polyimide films without use of the rubbing technique', Liquid Crystals, 17: 6, 847 — 854

To link to this Article: DOI: 10.1080/02678299408035477

URL: http://dx.doi.org/10.1080/02678299408035477

LIQUID CRYSTALS, 1994, VOL. 17, NO. 6, 847–854

Hysteresis behaviour of the nematic–cholesteric phase transition for liquid crystals on polyimide films without use of the rubbing technique

by YOSHIKAZU YABE*† and DAE-SHIK SEO‡

† Development Engineering Department, Engineering Division,
Fujitsu Kiden Limited, 1776 Yanokuchi, Inagi-shi, Tokyo 206, Japan
‡ Division of Electronic and Information Engineering,
Faculty of Technology, Tokyo University of Agriculture
and Technology, 2-24-16 Nakamachi, Koganei, Tokyo 184, Japan

(*Received 14 April 1993; in final form 9 February 1994; accepted 19 March 1994*)

The hysteresis behaviour of the nematic–cholesteric phase transition in liquid crystals is closely connected with the alignment of the liquid crystal molecules on the surfaces of treated solid substrates. We have investigated the hysteresis as a function of rubbing strength, using rubbing technology that controls the orientation of the liquid crystal molecules. The surface alignment direction contributes to the hysteresis width, is not dependent on rubbing strength, and is only slightly related to pretilt angles. A no-rubbing treatment, that is, random alignment, is important in order to create a large hysteresis width on homogeneously aligned polyimide films.

1. Introduction

The electrically induced nematic–cholesteric phase transition (NCPT) for an appropriate liquid crystal (LC) is a well known phenomenon, and it has been used for several types of LC displays such as light scattering [1, 2], White–Taylor [3] and bistable memory types [4–6]. The threshold electric field from cholesteric to nematic phase was derived by de Gennes [7] and that from nematic to cholesteric phase was derived by Greubel [8], and they discussed the dependence on the elastic constants and the helical pitch of the LC material. Lin-Hendel [9, 10] discussed the influences of the electric field-induced texture and phase change behaviour of dye-doped, long pitch, cholesteric, liquid crystal films as a function of boundary conditions, materials, and LC thickness-to-helical pitch ratio (*d*/*p*), using the anisotropic colour-absorption properties of the dichroic dye dopant.

We have investigated the bistable memory effect of the electric field-induced NCPT phenomenon for application in a projection display using the light scattering effect [11–13]. This display needs no polarizers, and so a high luminance image is obtained. Also the absence of light absorption without polarizers makes it possible to maintain a constant temperature on the LC display pad; thus the image quality preserves the same level even after several hours of continuous running. Moreover, the NCPT mode uses the memory effect of the LC, and the information content has no limitation,

---

* Author for correspondence.

theoretically. In order to keep this display drive stable, it is important that the width of the electro-optical hysteresis is large and is stabilized against the temperature.

A study of the dependence of the hysteresis behaviour in a NCPT-LC on the surface alignment effect, using a rubbing technique [14–16] that controls the direction of the LC molecules, has not yet been reported. The purpose of the present work was to obtain a relationship between the hysteresis width and the rubbing treatment on polymide (PI) films.

2. Hysteresis effects and the addressing scheme of a NCPT-LC

A NCPT-type LC with positive dielectric anisotropy changes state when the applied voltage is increased, as shown in fig. 1. It changes from a cloudy state, the cholesteric phase F, to a transparent state, the nematic phase H. When the voltage is decreased, it transforms from phase H to a metastable transparent state, nematic phase H′, then to phase F. In phase F, the LC in the panel has the helical structure. Because the axis of the helix is parallel to the glass substrates, incident light is scattered, making phase F cloudy. In phase H, the LC has no helical structure, but instead has a homeotropic structure. Incident light passes through the homeotropic structure, making phase H transparent. In phase H′, the structure of the LC is homeotropic, but in the centre of the layer the LC molecules are assumed to be slightly inclined. Phase H′ is a metastable homeotropic state. The hysteresis effect is thought to be affected by the specific balance between surface anchoring and the thermal properties of the helical structure.

The width of the hysteresis effect is designated the width of hysteresis, Δ, as shown in figure 1, i.e. the difference between the voltage V_u^{10}, which gives 10 per cent transmittance for cholesteric–nematic phase transitions and the voltage V_d^{90}, which gives 90 per cent transmittance for nematic–cholesteric phase transitions. The drive voltage, V_d, is set between V_u^{10} and V_d^{90}, as shown in figure 1.

NCPT type hysteresis enables the following four-stage addressing scheme. The first stage is initialization for writing. Applying twice V_d changes all pixels from state F to

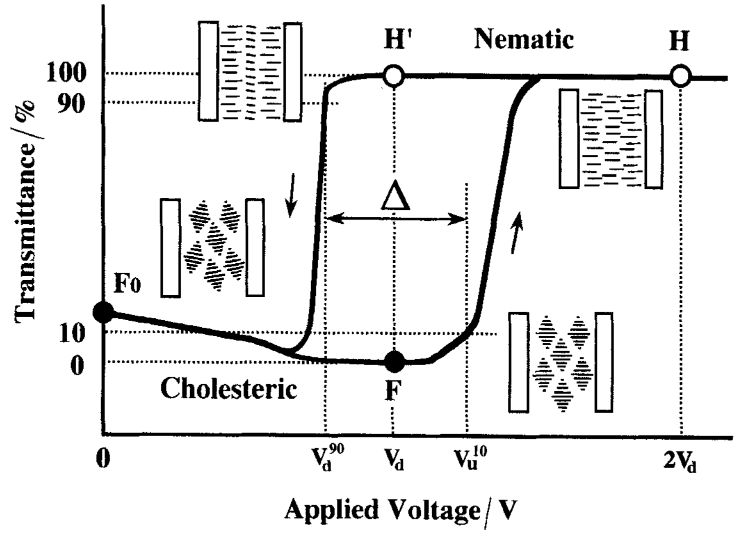

Figure 1. The phase transition and transmittance change for the NCPT-LC and a definition of hysteresis width, Δ.

state H. The second stage is writing using selected pixels. The selected pixels are changed to state F by removing voltages and then again applying the drive voltage (V_d). The third stage is writing at non-selected pixels. The non-selected pixels are maintained in state H′ or state H by continuing application of the drive voltage V_d or twice V_d. The fourth stage is maintaining the written images. The selected and non-selected pixels are maintained by applying the drive voltage.

3. Experimental

3.1. *Sample cells for measuring the hysteresis behaviour*

The glass plates were coated with indium–tin-oxide (ITO). Another layer on top of this is the PI film (RN-305, supplied from Nissan Chemical Industries Co., Ltd.) applied using the spin-coating method; it has a homogeneous alignment. It was polyimidized thermally at 230°C for 1 hour. The NCPT-LC layer had a thickness of 5·0 ± 0·1 μm, achieved using polymer beads for spacers, and checked using an LC layer thickness meter made by Otsuka-Electronics Co., Ltd.

We used a commercially available mixture as the nematic component (RDP-90613, Rodic Co., Ltd.), and a chiral dopant as the chiral nematic component (CNL-662, Asahidenka Co., Ltd.), as shown in figure 2. The helical pitch of the cholesteric phase was 1·0 μm using a 9 : 1 ratio of nematic to chiral nematic LC components. Helical pitches were measured using the Cano method [17]. The relationship between LC thickness and helical pitch was determined by the scattering intensity, using a driving voltage, ± 13 V max, that is able, using general CMOS-LSI, to drive the bistability of the hysteresis effect. The anisotropy of the refractive index (Δn) of the nematic component was 0·208 (20°C, 589 nm) in order to obtain the optical retardation of the NCPT-LC panel. The rotational viscosity of the nematic component was 27 cp (20°C). The phase transition temperature from nematic to isotropic phase of the nematic component was 85°C.

We used a rubbing technology that controls the surface alignment direction of the LC molecules and the rubbing direction was antiparallel for the two substrates. We prepared three kinds of cells—both sides unrubbed, one side rubbed and both sides rubbed—and also changed the rubbing strength (*M*).

3.2. *Control of rubbing strength*

Rubbing was done with a rotating cylinder, covered with a fabric consisting of vertical nylon threads of length 1·75 mm and 1·0 denier (Yo-15-N, Yoshikawa Chemical Industries Co., Ltd.), and allowing control of the separation between the base of the fabric and the surface of the ITO-coated glass plate coated with the PI films.

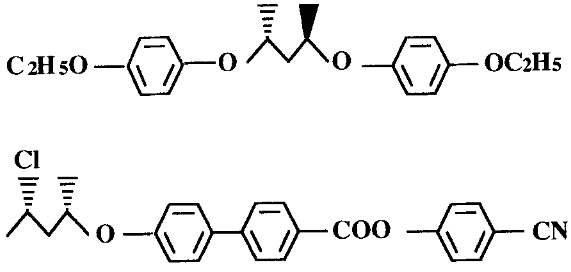

Figure 2. Structures of the chiral nematic LCs.

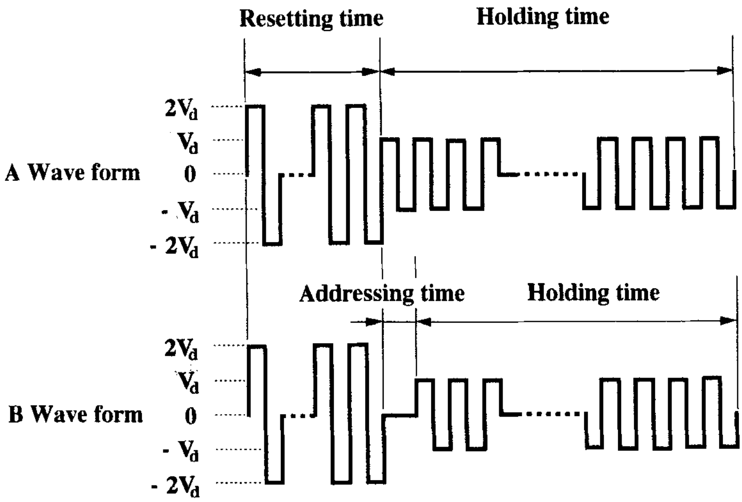

Figure 3. Schematic of the driving method. (*A*) Measuring wave form; the phase transition from cholesteric to nematic. (*B*) Measuring wave form; the phase transition from nematic to cholesteric.

The rubbing strength that is the most important parameter of the rubbing strength formula [18, 19] was increased by narrowing this clearance, thus increasing the rubbing pressure.

3.3. *Hysteresis behaviour measurements*

Measurement of the hysteresis, as shown in figure 1, was carried out using the scheme for driving of the device. The driving schematic, as shown in figure 3, is a special driving method for NCPT type LC, using the memory effect. Addressing time (t_r) is one pulse width (4 ms). Resetting time is t_r for 30 pulses. Holding time is t_r for 2501 pulses for the cholesteric–nematic phase transition and t_r for 2500 pulses for the nematic–cholesteric phase transition. The measurement temperature for the hysteresis behaviour was 30°C.

3.4. *Pretilt angle measurements*

In order to measure the pretilt angle (θ), we used the crystal rotation method [20]. The measurements were performed at 30°C. We used the same PI and LC material, but the LC material was the non-chiral nematic component and cells were prepared by assembling the substrates with antiparallel rubbing directions and also the rubbing strength was changed. The LC layer thickness was $60 \pm 0{\cdot}3\,\mu$m. We changed the thickness relative to that for the cell used for measuring the hysteresis behaviour in order to measure quickly and correctly the relationship between the rubbing strength and pretilt angle.

4. Results and discussion

4.1. *Relationship between pretilt angle and rubbing strength*

Figure 4 shows the dependence of the pretilt angle upon the rubbing strength on the PI films. In the case of both sides unrubbed, the pretilt angle is 0 degrees, because the LC molecules have a random alignment. In the case of both sides rubbed, the pretilt angle gradually increases and becomes about 5 degrees at $M = 1{\cdot}1$ mm; the pretilt angle

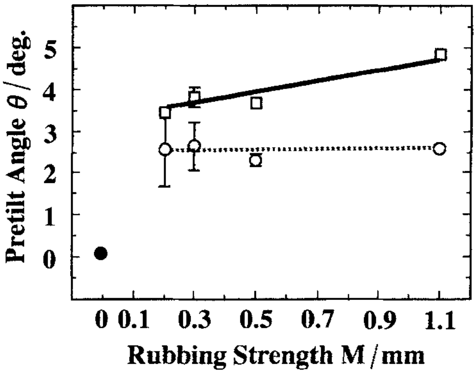

Figure 4. The dependence of the pretilt angle, θ, on the rubbing strength, *M*, used on the polymide films. (—□—), both sides rubbed; (---○---), one side rubbed; (●), both sides unrubbed.

is therefore directly related to the rubbing strength. In the case of one side rubbed, the pretilt angle does not depend on the rubbing strength and is almost constant at about 2·5 degrees. One side has random alignment and the other side is aligned, and so the rubbed side gives the average pretilt angle. It is also an interesting result that the rubbed side formed a good LC molecular alignment. In the case where the rubbing strength is raised to 1·2 mm, the PI alignment film is removed from the glass plate, and the result is that the pretilt angle decreases to 0 degree. It is considered that the rubbing effect is induced by a plastic flow of the polymer in its surface region, resulting in the unidirectional alignment of the main chains of the polymer [21, 22]. We used PI films that have these properties.

4.2. *Relationship between hysteresis width and rubbing strength*

Figure 5 shows the relationship between the hysteresis width and the rubbing strength. When both sides are unrubbed, the widest Δ is obtained. When both sides are rubbed, a Δ value is scarcely generated. In the case of one side rubbed, a comparatively large Δ is obtained. The most important point in this figure is that the hysteresis width is not related to the rubbing strength; that is, the hysteresis width is also not related to the pretilt angle. A random surface alignment impedes the phase transition.

4.3. *The electro-optical hysteresis properties for the three kinds of cells*

Figure 6 shows the electro-optical hysteresis properties for the three kinds of cells. Rubbing strength is constant at 0·5 mm. The measuring temperature is 30°C. Hysteresis width is decreased for the rubbed cells. The cholestric–nematic phase transition curve is moved in the direction of low applied voltage for one side rubbed. This result suggests that the cholesteric–nematic phase transition is affected by the orientation at the surface of the PI films and is induced by the electric field. The imbalance of having one side rubbed impedes the nematic–cholesteric phase transition and maintains a large hysteresis width. For both sides rubbed, the cholesteric–nematic phase transition curve is also moved in the direction of low applied voltage, but the nematic–cholesteric phase transition curve is moved in the direction of high applied voltage. This result suggests that the nematic–cholesteric phase transition is affected by the orientation at both sides. In both cases, the orientation at the surface of the PI films assists this phase transition.

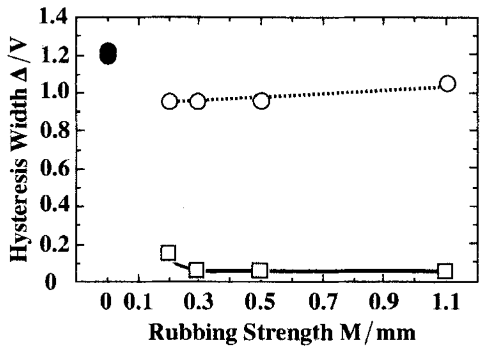

Figure 5. The relationship between the hysteresis width, Δ, and the rubbing strength, *M*, used on the polymide films. (—□—), both sides rubbed; (- - -○- - -), one side rubbed; (●), both sides unrubbed.

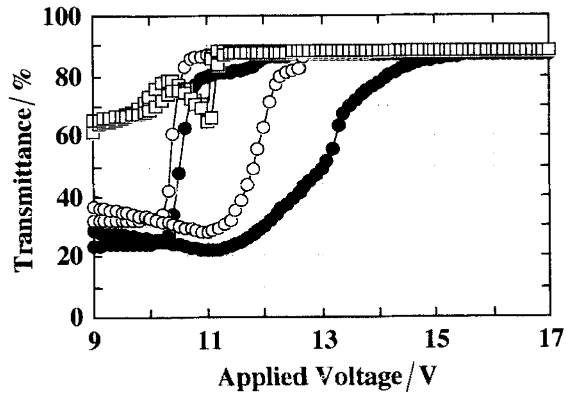

Figure 6. The electro-optical hysteresis properties of the three kinds of cells. *M* = 0·5 mm. (□), both sides rubbed; (○), one side rubbed; (●), both sides unrubbed.

4.4. *The temperature dependence of hysteresis width*

The temperature dependence of the hysteresis width for the three kinds of cells is shown in figure 7. Rubbing strength is constant at 0·5 mm. At a measuring temperature of 30°C and with both sides unrubbed a large hysteresis width is obtained, and is constant over a wide temperature range. A large hysteresis width is not obtained with both sides rubbed. One side rubbed gives a decreasing hysteresis with up to 40°C. It is considered that the direction of surface alignment and the thermal properties of the LC are important to inducing the phase transition easily. These results are not altered with changing the rubbing strength.

4.5. *The relationship between the hysteresis width and the pretilt angle*

Figure 8 shows the relationship between the hysteresis width and the pretilt angle on the PI films. Hysteresis width does not depend on the pretilt angle for any of the three kinds of cell. Because the liquid crystal has a chiral structure, the bulk-LC molecular alignment will be only slightly related to the pretilt angles. The generation of hysteresis is closely related to the surface alignment direction rather than to the pretilt angle.

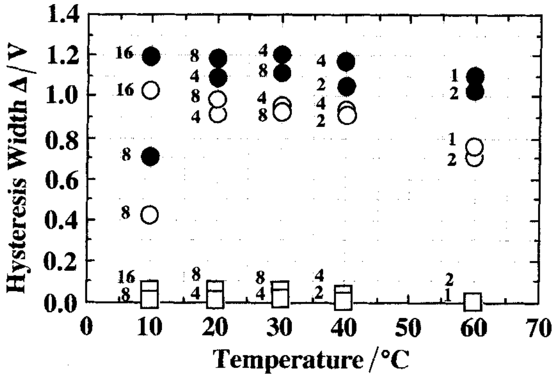

Figure 7. The temperature dependence of the hysteresis width, Δ. The numerical values in this figure indicate the addressing time. $M = 0{\cdot}5$ mm. (□), both sides rubbed; (○), one side rubbed; (●), both sides unrubbed.

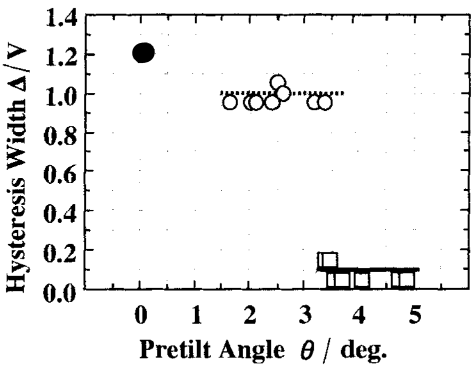

Figure 8. The relationship between the hysteresis width, Δ, and the pretilt angle, θ, on the polymide films. (—□—), both sides rubbed; (---○---), one side rubbed; (●), both sides unrubbed.

5. Conclusions

The generation of the hysteresis width is closely connected with the surface alignment direction and is not dependent on the rubbing strength. Changing the pretilt angle also does not affect the hysteresis width. A no-rubbing treatment is very important in order to create a wide hysteresis width over a wide temperature range, and a random homogeneous surface alignment can induce a large hysteresis width.

References

[1] Wysocki, J. J., Adams, A., and Haas, W., 1968, *Phys. Rev. Lett.*, **20,** 1024.
[2] Heilmeier, G. H., and Golgmacher, J. E., 1968, *Appl. Phys. Lett.*, **13,** 132.
[3] White, D. L., and Taylor, G. N., 1974, *J. appl. Phys.*, **45,** 4718.
[4] Heffner, W. R., .and Berreman, D. W., 1982, *J. appl. Phys.*, **53,** 8599.
[5] Kawachi, K., Kato, K., and Kogure, O., 1977, *Jap. J. appl. Phys.*, **16,** 1673.
[6] Kawachi, K., Kato, K., and Kogure, O., 1977, *Jap. J. appl. Phys.*, **16,** 1263.
[7] de Gennes, P. G., 1968, *Solid St. Commun.*, **6,** 163.
[8] Greubel, W., 1974, *Appl. Phys. Lett..*, **25,** 5.
[9] Lin-Hendel, C. G., 1981, *Appl. Phys. Lett.*, **38,** 615.
[10] Lin-Hendel, C. G., 1982, *J. appl. Phys.*, **53,** 916.

[11] Mochizuki, A., Gondo, H., Watanuki, T., Saito, K., Ikegami, K., and Okuyama, H., 1985, *Proc. SID*, **26,** 243.

[12] Mochizuki, A., Yoshiuhara, T., Iwasaki, M., Yamagishi, Y., Koike, Y., Haraguchi, M., and Kaneko, Y., 1990, *Proc. SID*, **31,** 1888.

[13] Yabe, Y., Yamada, H., Hoshi, T., Yoshihara, T., Mochizuki, A., and Yoneda, Y., 1993, *J. Soc. Inf. Dis.*, **1,** 43.

[14] Becker, M. E., Kilian, R. A., Kosmowski, B. B., and Milynsk, D. A., 1986, *Molec. Crystals liq. Crystals*, **130,** 167.

[15] Geary, J. M., Goodby, J. W., Kmetz, A. R., and Patel, J. S., 1987, *J. appl. Phys.*, **62,** 4100.

[16] Kuniyasu, S., Fukuro, H., Maeda, K., Nitta, M., Ozaki, N., and Kobayashi, S., 1988, *Jap. J. appl. Phys.*, **27,** 827.

[17] Cano, R., 1968, *Bull. Soc. fr. Minér. Cristallogr.*, **91,** 20.

[18] Uchida, T., Hirano, M., and Sasaki, H., 1989, *Liq. crystals*, **5,** 1127.

[19] Seo, D.-S., Muroi, K., and Kobayashi, S., 1992, *Molec. Crystals liq. Crystals*, **213,** 223.

[20] Scheffer, T. J., and Nehring, J., 1977, *J. appl. Phys.*, **48,** 1783.

[21] Aoyama, H., Yamazaki, Y., Matsuura, N., Mada, H., and Kobayashi, S., 1981, *Molec. Crystals liq. Crystals*, **72,** 127.

[22] Yokoyama, H., and van Sprang, H. A., 1985, *J. appl. Phys.*, **57,** 4520.